Conductance quantization in V-groove quantum wires

D. Kaufman, Y. Berk, B. Dwir, A. Rudra, A. Palevski,* and E. Kapon
Department of Physics, Swiss Federal Institute of Technology (EPFL), CH-1015 Lausanne, Switzerland
(Received 8 July 1998)

We have observed and studied ballistic one-dimensional (1D) electron transport in V-grooved GaAs-$Al_xGa_{1-x}As$ heterostructures. In two different regimes of quantum wire confinement the conductance varies in a steplike manner, with the number of populated 1D subbands controlled by a gate voltage. For weak lateral confinement, the conductance steps nearly attain the $2e^2/h$ value, whereas for stronger confinement the values of the conductance steps are suppressed. Our results suggest that a poor coupling between the 1D states of the wire and the 2D states of the reservoirs outside the gated region is responsible for the conductance suppression for strong lateral confinement. [S0163-1829(99)50516-X]

Electron transport in one-dimensional (1D) systems has been extensively studied both experimentally and theoretically.[1,2] The most striking feature of 1D transport is revealed in the ballistic limit, where the conductance is quantized in units of $G_0 \equiv 2e^2/h$.[3] This quantization has been observed in two-dimensional electron gas (2DEG) systems further confined to 1D by means of an electrostatic potential in a point contact geometry.[4] In these structures, the 1D electron channels are adiabatically connected to the 2D electron reservoirs. However, other structures, which use ''rigid'' confinement potential (e.g., etched stripe structures,[5] overgrown constrictions,[6] and T-shaped cleaved-edge overgrown wires[7]), all show ballistic quantized conductance that significantly deviates from the G_0 values. Several explanations have been suggested for the origin of these deviations, most notably invoking electron-electron interaction[5,8] and contact resistance effects.[7,9] Additional ''anomalous'' conductance features have been reported for both point contacts[10] and rigid potential structures,[6,11] which showed spurious features at various fractional values (0.5,0.7,0.2) of G_0. The origin of these fractional-G_0 features has been attributed to zero-magnetic-field spin polarization due to electron-electron interaction.[6,10,12]

In this paper we report the results of electron-transport measurements in V-groove GaAs/$Al_xGa_{1-x}As$ quantum wires (QWR's). With these structures, it is possible to control the strength of the lateral quantum confinement, thus allowing the comparison between nearly adiabatic and more abrupt transitions between the wire and the reservoir regions. In the ballistic transport regime, obtained for wires shorter than ~ 1.5 μm, we observe a systematic increase in the deviation of the conductance steps from G_0 as the strength of the lateral confinement increases. Our data support recent models[7,9] assigning these deviations to electron scattering at the interface between the 2D contacts and the 1D wires. Furthermore, our study suggests that the deviation of the conductance steps from the G_0 values and the anomalous fractional-G_0 features are of different origins.

Our GaAs/$Al_xGa_{1-x}As$ QWR's were grown by low-pressure organometallic chemical-vapor deposition on undoped (100)-GaAs substrates patterned with 3-μm-pitch, $[01\bar{1}]$-orientated V grooves (see Ref. 13 for details of the growth and fabrication). The conducting region consisted of a GaAs quantum well (QW) layer sandwiched between $Al_{0.3}Ga_{0.7}As$ barriers, modulation doped on both sides with Si. The nominal QW thickness $t_{\rm nom}$ was varied in different samples between 7 and 26 nm. The growth on the corrugated surface results in the formation of a crescent-shaped GaAs QWR of center thickness $\sim 1.6t_{\rm nom}$ as well as sidewall and top QW's on the slopes of the grooves and the top of the ridges between the channels [see transmission electron microscope cross section in Fig. 1(a)]. The 2DEG on the sidewalls is connected to the 1DEG at the wire via constrictions. For the samples with a thinner QW layer, the thinner crescents yield stronger lateral confining potential (CP) due to the GaAs layer tapering.[14] In addition to this ''rigid'' confinement, the V-shaped doped regions result in softer, electric-field induced lateral confinement[15] that becomes the dominant one for thicker GaAs layers.

Conductance measurements of the 2DEG in the QW parts of the structure were performed using Hall bar geometry samples made by depositing Au/Ge/Ni Ohmic contacts on 10-μm-wide mesas oriented parallel or perpendicular to the V grooves. For isolation of the QWR contribution to the conductance, narrow mesas incorporating a single QWR groove and Ti/Au Schottky gates were fabricated using electron-beam lithography (see Ref. 13 for details). A scanning electron micrograph (SEM) view of such a QWR device is shown in Fig. 1(b). The devices were measured in a variable-temperature cryostat (1.4–300 K) using a lock-in four-terminal technique with 10-nA ac excitation current. About 100 QWR devices were studied and the results discussed here represent the general trends observed.

From low-field Hall effect, Shubnikov–de Haas magnetoresistance oscillations, and carrier depletion measurements, we established the transport parameters for the 2DEG. The electron density in the sidewalls ($5-9\times10^{11}\,{\rm cm}^{-2}$ in different samples) is higher by $\sim$30% than in reference samples grown on planar (001) GaAs substrates, while the sidewall mobility is similar to that of planar samples. We observed a distinct anisotropy between resistance measured parallel and perpendicular to the V grooves, which steeply increases with decreasing QW thickness. The origin of this anisotropy was proved to originate only from the bottom of the groove, con-

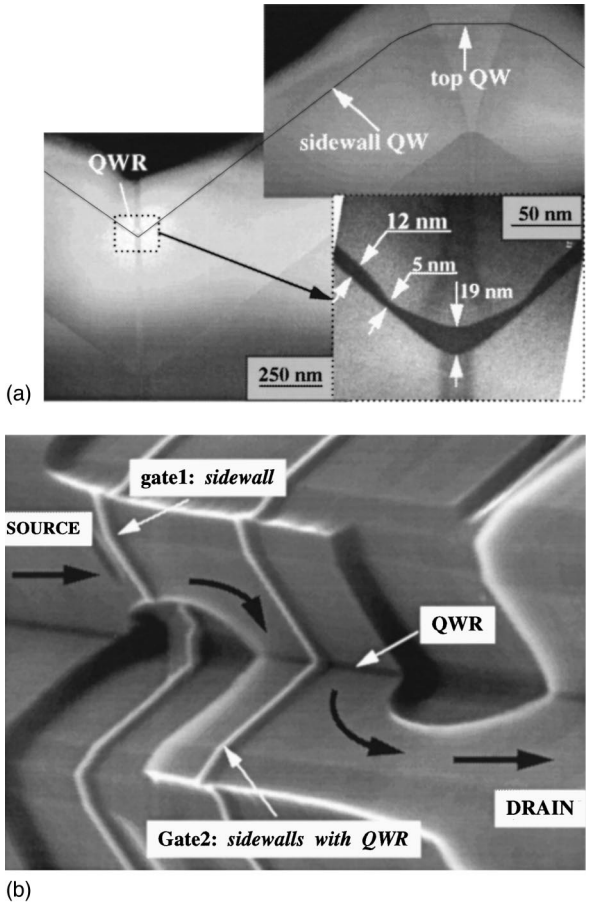

FIG. 1. (a) Cross-sectional TEM images of a QWR heterostructure with nominally 12-nm-thick GaAs layer. The sidewall QW, top QW, and QWR regions are indicated. Inset: a magnified view of the QWR region with indication of the GaAs layer dimensions. (b) SEM image (tilted 75° to the surface) of the S-shape device. Black arrows indicate the trajectory of the current flow: from source to drain through the ''sidewall-wire-sidewall'' sequence. Two metallic gates of 0.25 μm width each are deposited, one on the sidewall area only, the other on the full ''sidewall-wire-sidewall'' path.

sistent with the constrictions next to the QWR [Fig. 1(a)], which produce a strong potential barrier there.

Because of the difficulty in contacting the QWR's directly, we have employed the 2DEG on the groove sidewalls as electron reservoirs in a two-terminal configuration. To isolate the QWR section between these reservoirs, we used a negatively biased Schottky metal gate of length L_g, across a mesa containing a single V groove, to deplete carriers from the sidewall QW.[16] Due to the electrostatics of the V-groove capacitor geometry, the depletion of carriers occurs first at the sidewalls, and only subsequently at the QWR. Numerical simulations indicate that the average electric field at the bottom of the V groove is about 10% of its value in the sidewalls, as long as there are carriers in the sidewalls. The sequential depletion of carriers is readily demonstrated using the S-shaped mesa device of Fig. 1(b). The current is forced to pass from one sidewall QW, through the QWR, to the other sidewall QW. Two separate gates are placed so that one depletes only a QW sidewall, whereas the other depletes both sidewall QW's and the QWR. The dashed curve in the inset of Fig. 2 shows the device conductance as a function of

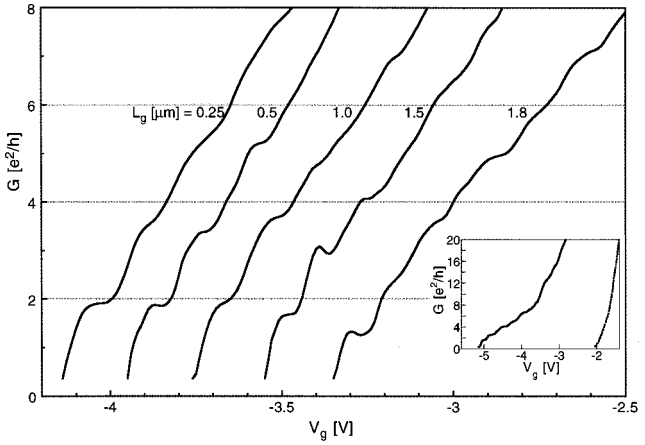

FIG. 2. Conductance vs gate voltage for $t_{\mathrm{nom}}=26$ nm at 4.2 K. The different curves represent gate widths L_g from 0.25 to 1.8 μm. The inset shows the conductance vs gate voltage for $t_{\mathrm{nom}}=21$ nm and $L_g=0.5$ μm at 4.2 K; The solid curve corresponds to gating of the sidewalls and the QWR, while the dashed line is for gating of the sidewalls only.

the sidewall gate voltage, revealing complete depletion at $V_g\sim-2$ V. The solid curve, corresponding to the second type of gate, shows complete depletion only at a more negative voltage, $V_g\sim-5$ V. The conductance measured at gate voltages below -2 V is thus solely attributed to the QWR region. The conductance variation in this gate voltage regime is shown in Fig. 2 for different values of gate length L_g. The steplike structure indicates sequential depopulation of the 1D subbands in the QWR, and repeats in all our samples.

The dependence of the QWR conductance (resistance) on gate length is summarized in Fig. 3. The measured variation of the resistance at the first step $R_1=1/G_1$ as a function of L_g up to 8 μm is shown in the main part of Fig. 3. The linear variation of R with L_g, for $L_g>2$ μm (solid line), is typical of diffusive transport. However, for L_g shorter than $\sim$1.5 μm, a saturation of the resistance is evident. The inset of Fig.

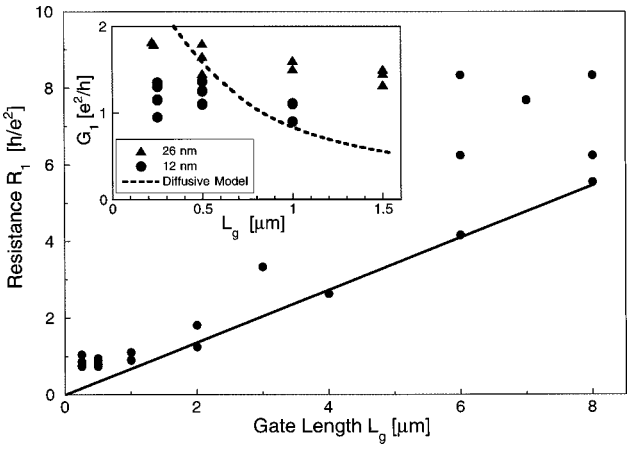

FIG. 3. Resistance value R_1 of the first step as function of gate length, for samples with $t_{\mathrm{nom}}=12$ nm. The solid line represents linear gate length dependence, fitted to the best conductance values for gates longer than 2 μm. The inset shows details of the weak gate length dependence of the conductance at short gate lengths for $t_{\mathrm{nom}}=12$ and 26 nm. The dashed line represents a simplified model of diffusive transport.

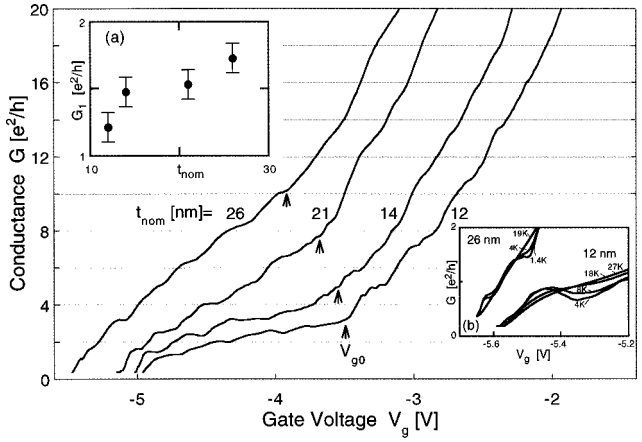

FIG. 4. Conductance vs gate voltage for $L_g = 0.5\,\mu$m at 4.2 K, for nominal QW thickness of 12, 14, 21, and 26 nm. Insets: (a) Average value (over several samples, for $L_g = 0.5\,\mu$m and at 4.2 K) of the first conductance step for different QW thicknesses $t_{\rm nom}$. (b) Conductance vs gate voltage for $L_g = 0.5\,\mu$m at different temperatures and for $t_{\rm nom} = 12$ and 26 nm.

3 shows the conductance value of the first step G_1 for gate lengths in the range 0.25–1.5 μm for two different values of $t_{\rm nom}$, 12 and 26 nm. In this short gate regime, the length dependence is much weaker than is expected in the case of diffusive transport [dashed line in the inset of Fig. 3 (Ref. 17)]. Note that the value of the conductance step is systematically lower for $t_{\rm nom} = 12$ nm than for 26 nm. The weak dependence of the conductance for QWR segments shorter than $\sim$1.5 μm thus indicates ballistic transport in this regime.[2]

The dependence of the conductance on the QWR thickness is shown in Fig. 4 for four different values of $t_{\rm nom}$. A common feature for all the curves in is an abrupt change of the slope dG/dV_g at certain values V_{go} (denoted by arrows). This change in slope is larger for structures with smaller $t_{\rm nom}$. Moreover, the conductance step values in the region of $V_g > V_{go}$ are closer to G_0, whereas the values of the steps in the region $V_g < V_{go}$ are suppressed, and more strongly so for lower $t_{\rm nom}$. In inset (a) of Fig. 4 we plot the value of the first step G_1, averaged over more than 20 devices, versus $t_{\rm nom}$. The deviation of the average values of G_1 (for each $t_{\rm nom}$) from the canonical value G_0 is more significant than the standard deviation of the measured values. As $t_{\rm nom}$ increases, the conductance approaches G_0, and the highest value of G_1 that we measured (for $t_{\rm nom} = 26$ nm) is $0.95G_0$. The variation of the conductance curves with temperature, inset (b) of Fig. 4, shows the gradual smearing of the step structure as the temperature increases. This smearing occurs at a lower temperature for the sample with larger $t_{\rm nom}$, consistent with a weaker CP in that case. We also note in this inset a conductance feature around $0.5G_1$, for both values of $t_{\rm nom}$. Such features can also be observed in some of the traces in Figs. 2 and 4; they were observed in about 50% of our samples, and the feature conductance value varied between 0.3 to $0.8G_1$. No systematic dependence of the feature on $t_{\rm nom}$ was observed.

The measured 2D mobility in our structures (as large as 2.5×10^5 cm^2/V s) implies an electron mean free path of up to 2 μm. In separate atomic force microscopy studies,[18] we have shown that the V-groove wires exhibit monolayer-smooth interfaces within wire segments up to 1–2 μm long. Both observations are consistent with our conductance results, which show a ballistic transport regime for gates shorter than $\sim$1.5 μm. Assuming that the gate capacitance of the wire does not change abruptly with V_g, we attribute the change of slope in Fig. 4 (at $V_g = V_{go}$) to an abrupt change in 1D subband separation. Using the approximation that the Fermi energy varies linearly with gate voltage, we obtain $dG/dV_g \propto dG/dE_F \propto dG/\varepsilon dN \propto 1/\varepsilon(2e^2/h)$, where N is the carrier density and ε is the 1D subband energy separation. For $V_g > V_{go}$, the electron states that are depleted by the gate are associated with wave functions that spread well into the sidewalls. These have a relatively small ε, determined mainly by the CP due to the electrostatic field in the V-groove capacitor.[15] However, at more negative gate voltages, the states which are depleted are more confined at the bottom of the V groove, and their energy spacing, defined primarily by the QWR built-in CP, is larger. The slope change in Fig. 4 is less abrupt for larger $t_{\rm nom}$, in accordance with a weaker built-in CP, which is essentially dominated by the electrostatic V-groove CP for $t_{\rm nom} = 26$ nm. Analysis of the temperature dependence of the conductance curves, inset (b) of Fig. 4, supports this picture. If we assume that the effect of temperature is equivalent to an averaging with $\varepsilon \approx 4k_BT$, the temperature at which all conductance features disappear for $t_{\rm nom} = 26$ nm corresponds to an estimated value of $\varepsilon \sim 2.5$ meV. For $t_{\rm nom} = 12$ nm, the smearing of the higher steps ($V_g > V_{go}$) is observed at the same temperature as for $t_{\rm nom} = 26$ nm, while the lower steps disappear only at a higher temperature, yielding $\varepsilon \sim 5$ meV.

The suppression of the lower conductance steps, as seen in Fig. 4 and inset (b), could be attributed to several mechanisms. As $t_{\rm nom}$ decreases (and ε increases), the deviation of the steps from the canonical values is stronger. It can be explained as due to poor coupling of the QWR states to the 2DEG ones, which act as a reservoir in our two-terminal measurement. This is unlike the adiabatic 2D-1D coupling achieved in point contacts.[4] Electrons under the gate, which are in a 1D subband with a large separation ε, stay in the same 1D subband even far away from the gated region. Therefore, in spite of the fact that the movement of the electrons is ballistic under the gated region, their poor coupling to the 2DEG leads to backscattering, increasing the observed two-terminal resistance. Such a model was also considered by Yacoby *et al.*,[7] as a possible explanation for the noncanonical values of conductance steps observed in T-shaped wires. Our QWR electronic states resemble those in T-shape wires,[7] in the sense that both have inherent quantum confinement that extends throughout the entire sample. Since each of the 1D states has different coupling to the 2DEG, the resulting contact resistance cannot be simply described as a unique factor. However, in our structures there exist additional (higher-energy) 1D states under the gate, which resemble those in point contacts, and which more adiabatically evolve into 2D states in the 2DEG, away from the gate. Those higher order states are probably responsible for the larger value of dG/dV for $V_g > V_{go}$ (Fig. 4). As $t_{\rm nom}$ increases, the built-in CP becomes weaker, and the subband

spacing decreases. Thus, the electrons are better coupled to the 2DEG, which increases the value of the conductance steps towards the canonical value, and the slope change of the $G(V_g)$ curve becomes smaller. Alternatively, a recent model[9] proposes Friedel oscillations of the density of states in the 2DEG close to the QWR interface, leading to enhanced backscattering there, as the source of noncanonical values of conductance steps. Our results, although not in contradiction with this picture, do not allow to distinguish between the two alternative models.

The conductance features observed in many of our samples at $0.3-0.8G_1$, appear to be independent of the noncanonical values of conductance steps. It is thus likely that their origin is different, possibly related to electron spin polarization as proposed for similar features observed in adiabatic point contacts.[12] Our study therefore shows that conductance steplike features different from the canonical values can result from either reservoir mismatch effects or other, spurious effects, e.g., the spin polarization effects proposed earlier. The observation of a deviation from G_0 cannot by itself determine the origin of the mechanism for such ''anomalous'' behavior; rather, the full evolution of the conductance features with system parameters is necessary to distinguish step suppression due to 1D-2D mismatch from other conductance features.

To summarize, we measured the conductance properties of doped V-groove QWR's by applying a negatively biased gate over the structure. The sequential depletion of the 2DEG and the QWR allows us to make electrical contacts to the QWR via the 2DEG. In the 1D conductance regime, we observed conductance steps evidencing the ballistic nature of the QWR's with a gate length of up to ~ 1.5 μm. The step values are lower than $2e^2/h$ by a factor that depends on the QWR thickness. This dependence is related to the presence of a stronger built-in confinement potential in the thin QWR's (5 meV at $t_{\mathrm{nom}}=12$ nm vs 2 meV at $t_{\mathrm{nom}}=26$ nm). Our studies indicate that the suppression of the step values arises from electron scattering at the 2DEG-QWR interface, in agreement with recent models of backscattering and Friedel oscillations at this boundary.

We wish to thank K. Leifer for tunneling electron microscopy (TEM) analysis and D. Crisinel for numerical simulations. Support from Fond National Suisse de la Recherche Scientifique and the German–Israeli Foundation are gratefully acknowledged.

*Permanent address: School of Physics and Astronomy, Raymond and Beverly Sackler Faculty of Exact Sciences, Tel Aviv University, Tel Aviv 69978, Israel.

[1] D. K. Ferry and S. M. Goodnick, *Transport in Nanostructures* (Cambridge University Press, Cambridge, U.K., 1997).

[2] Y. Imry, *Introduction to Mesoscopic Physics* (Oxford University Press, Oxford, U.K., 1997).

[3] R. Landauer, IBM J. Res. Dev. **1**, 223 (1957); Phys. Lett. **85A**, 91 (1981).

[4] B. J. van Wees, H. van Houten, C. W. J. Beenakker, J. G. Williamson, L. P. Kouwenhoven, D. van der Marel, and C. T. Foxon, Phys. Rev. Lett. **60**, 848 (1988); D. A. Wharam, T. J. Thornton, R. Newbury, M. Pepper, H. Ahmed, J. E. F. Frost, D. G. Hasko, D. C. Peacock, D. A. Ritchie, and G. A. C. Jones, J. Phys. C **21**, L209 (1988).

[5] S. Tarucha, T. Honda, and T. Saku, Solid State Commun. **94**, 413 (1995); Y. Takagaki, K. Gamo, S. Namba, S. Takaoka, and K. Murase, Appl. Phys. Lett. **57**, 2916 (1990).

[6] P. Ramvall, N. Carlsson, I. Maximov, P. Omling, L. Samuelson, W. Seifert, S. Lourdudoss, and Q. Wang, Appl. Phys. Lett. **71**, 918 (1997).

[7] A. Yacoby, H. L. Stormer, N. S. Wingreen, L. N. Pfeiffer, K. W. Baldwin, and K. W. West, Phys. Rev. Lett. **77**, 4612 (1996).

[8] D. L. Maslov, and M. Stone, Phys. Rev. B **52**, R5539 (1995); D. L. Maslov, *ibid.* **52**, R14 368 (1995); M. Ogata and H. Fukuyama, Phys. Rev. Lett. **73**, 468 (1994).

[9] A. Y. Alekseev and V. V. Cheianov, Phys. Rev. B **57**, R6834 (1998).

[10] K. J. Thomas, J. T. Nicholls, M. Y. Simmons, M. Pepper, D. R. Mace, and D. A. Ritchie, Phys. Rev. Lett. **77**, 135 (1996).

[11] A. Yacoby, H. L. Stormer, K. W. Baldwin, L. N. Pfeiffer, and K. W. West, Solid State Commun. **101**, 77 (1997).

[12] C. K. Wang and K. F. Berggren, Phys. Rev. B **54**, R14 257 (1996).

[13] B. Dwir, D. Kaufman, Y. Berk, A. Rudra, A. Palevski, and E. Kapon, Physica B **259–261**, 1025 (1999).

[14] E. Kapon, D. M. Hwang, and R. Bhat, Phys. Rev. Lett. **63**, 430 (1989); A. Gustafsson, F. Reinhardt, G. Biasiol, and E. Kapon, Appl. Phys. Lett. **67**, 3673 (1995).

[15] V. Trück, O. Stier, F. Heinrichsdorff, M. Grundmann, and D. Bimberg, Phys. Rev. B **55**, 7733 (1997); K. Vacek, A. Sawada, and T. Usagawa, Appl. Phys. Lett. **65**, 3096 (1994).

[16] A similar technique utilizing two separate gates, one for isolation and the other for depopulation 1D states, was employed in the T-shape QWR's of Refs. 7 and 11.

[17] The depleted wire length is somewhat shorter than the gate length L_g. Using numerical simulations of the V-groove electrostatics, we confirmed that this length difference does not change our results in a significant way, and it was taken into account when modeling the diffusive transport in the inset of Fig. 3.

[18] F. Reinhardt, G. Biasiol, and E. Kapon (unpublished).